

CRAMÉR-RAO BOUNDS AND ESTIMATION ALGORITHMS FOR DELAY/DOPPLER AND CONVENTIONAL ALTIMETRY

A. Halimi, C. Mailhes, J.-Y. Tournéret

University of Toulouse, IRIT-ENSEEIH-TéSA, Toulouse, France
2, rue Charles Camichel, 31071 Toulouse, France

ABSTRACT

Delay/Doppler radar altimetry has been receiving an increasing interest, especially since the launch of the first altimeter in 2010. It aims at reducing the measurement noise and increasing the along-track resolution in comparison with conventional pulse limited altimetry. A semi-analytical model was recently introduced for this new generation of delay/Doppler altimeters. The first contribution of this paper is the derivation of the Cramér-Rao bounds (CRBs) associated with the parameters of this recent delay/Doppler model. These bounds are then compared with those obtained for conventional altimetry. The second contribution of this paper is the derivation of a new weighted least squares estimator based on the semi-analytical delay/Doppler model. The performance of this estimator is very promising when compared to other more classical estimators and to the corresponding CRBs.

Index Terms— Cramér-Rao bounds, delay/Doppler map, least squares estimation, maximum likelihood estimation, SAR altimetry.

1. INTRODUCTION

The concept of delay/Doppler radar altimetry was introduced in [1]. However, more than 10 years were necessary to develop the first altimeter which was launched in 2010 with the Cryosat-2 satellite. Delay/Doppler altimeters aim at reducing the measurement noise and increasing the along-track resolution, i.e., reducing the observed surface in comparison with conventional pulse limited altimeters. Noise reduction is obtained by increasing the number of observations which allows a better estimation of the physical parameters of interest. The increase of resolution is achieved by using the information contained in the Doppler frequency (related to the satellite velocity). The resolution improvement can be advantageously exploited to process altimetric measurements closer to the coast. One can expect to extract useful information from oceanic cells located up to 300 meters from the coast whereas the minimum accepted distance is about 10 km for conventional altimetry (CA). The first part of this paper introduces the semi-analytical model for delay/Doppler altimetry (DDA) that was recently defined in [2, 3]. This model

expresses the altimetric waveform as a function of three parameters: the significant wave height SWH, the epoch τ (related to the distance between the satellite and the observed oceanic surface) and the amplitude P_u (related to the speed of the wind).

The first contribution of this paper is the derivation of the Cramér-Rao bounds (CRBs) of the parameters associated with the semi-analytic delay/Doppler altimetric model. These CRBs are then compared with the CA bounds in order to demonstrate the expected improvement of performance obtained with DDA. The second contribution of this paper is the study of a new weighted least-squares (WLS) estimator for the parameters of the semi-analytical delay/Doppler model. This estimator combines the good properties of the standard least-squares (LS) estimator [4, 5] (i.e., its reduced computational cost) and of the maximum likelihood estimator (i.e., reduced mean square errors for the estimates).

The paper is organized as follows. Section 2 describes the CA and DDA models investigated in this study. The CRBs associated with the parameters of these models are established in Section 3. Section 4 presents different methods for estimating the parameters of the CA and DDA models. In particular, a new estimator minimizing a WLS criterion is introduced. Simulation results are presented in Section 5. Conclusions and future work are finally reported in Section 6.

2. DATA MODEL

This section introduces the models considered for conventional and delay/Doppler altimetry.

2.1. Conventional altimetry

The conventional altimetric signal can be expressed as the convolution of three terms: the flat surface impulse response (FSIR), the probability density function (PDF) of the height of the specular scatterers and the point target response of the radar (PTR) as follows [6]

$$s_c(t) = \text{FSIR}(t) * \text{PDF}(t) * \text{PTR}_T(t) \quad (1)$$

with

$$\text{FSIR}(t) = P_u \exp\left[-\frac{4c}{\gamma h}(t - \tau_s)\right] U(t - \tau_s) \quad (2)$$

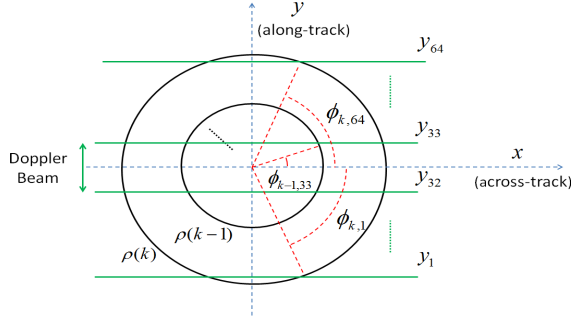


Fig. 1. Propagation circles (in black) and Doppler beams (in green) for conventional and delay/Doppler altimetry.

$$\text{PDF}(t) = \sqrt{\frac{2}{\pi}} \frac{c}{\text{SWH}} \exp\left(-2 \frac{c^2 t^2}{\text{SWH}^2}\right) \quad (3)$$

$$\text{PTR}_T(t) = \left| \frac{\sin\left(\frac{\pi t}{T}\right)}{\frac{\pi t}{T}} \right|^2 \quad (4)$$

where t is the time, τ_s is the epoch expressed in seconds, c is the speed of light, T is the time resolution, γ is an antenna beamwidth parameter, h is the minimum satellite-surface distance and $U(\cdot)$ denotes the Heaviside function.

2.2. Delay/Doppler altimetry

The mean power of a delay/Doppler echo can also be expressed as the convolution of three terms [7]. However, the power term depends on two dimensions, i.e, time and Doppler frequency [8], leading to

$$P(t, f) = \text{FSIR}(t, f) * \text{PDF}(t) * \text{PTR}(t, f) \quad (5)$$

with

$$\text{PTR}(t, f) = \text{PTR}_T(t) \text{PTR}_F(f), \quad \text{PTR}_F(f) = \left| \frac{\sin\left(\frac{\pi f}{F}\right)}{\frac{\pi f}{F}} \right|^2 \quad (6)$$

where F is the frequency resolution. The FSIR is obtained by integrating the energy contained in the intersection of the propagation circles with the $N = 64$ rectangular beams related to Doppler frequencies (see Fig. 1) [2, 3]

$$\begin{aligned} \text{FSIR}(t, n) &= \frac{P_u}{\pi} \exp\left[-\frac{4c}{\gamma h}(t - \tau_s)\right] U(t - \tau_s) \\ &\times [\phi_{t, n+1}(\tau_s) - \phi_{t, n}(\tau_s)] \end{aligned} \quad (7)$$

with

$$\phi_{t, n}(\tau_s) = \text{Re} \left[\arctan \left(\frac{y_n}{\sqrt{\rho^2(t - \tau_s) - y_n^2}} \right) \right] \quad (8)$$

where $n = 1, \dots, N$, $N = 64$ being the number of Doppler beams, $\rho(t) = \sqrt{hct}$ is the radius of the propagation circles, $y_n = \frac{h\lambda}{2v_s} f_n$ is the ordinate of the n^{th} Doppler beam,

$f_n = (n - 32.5) F$ is the n^{th} Doppler frequency (32.5 allows to obtain a central beam), v_s is the satellite velocity, λ is the wavelength and $\text{Re}(x)$ denotes the real part of the complex number x .

Eq. (5) provides a two dimension image known as delay/Doppler map. In order to obtain a “multi-look” altimetric waveform, a delay compensation operation is applied to each Doppler beam followed by the sum of these beams [1, 9]. The resulting multi-look delay/Doppler signal can be written $s_d(t) = \sum_{n=1}^N P(t - \delta t_n, f_n)$, where δt_n is the delay compensation expressed in seconds.

2.3. Comparison between CA and DDA waveforms

The altimetric signals $s_c(t)$ and $s_d(t)$ are classically sampled at time instants $t_k = kT$, for $k = 1, \dots, K$, where $K = 104$ is the number of samples. The epoch is then expressed as a “gate number” τ with $\tau_s = \tau T$. The resulting discrete signals denoted as $s_c = [s_c(1), \dots, s_c(K)]^T$ and $s_d = [s_d(1), \dots, s_d(K)]^T$ depend on the altimetric parameter vector $\theta = (\text{SWH}, \tau, P_u)^T$. Fig. 2 compares typical delay/Doppler (in blue) and conventional altimetric echoes (in red) for two values of SWH (SWH = 2 m and SWH = 8 m) and $(\tau, P_u) = (31, 1)$. It is interesting to note that the delay/Doppler echo has a peaky shape around the epoch because of delay compensation. Note also that the variation of SWH affects the form of the DDA echo while it only changes the slope of the CA echo around the epoch $\tau = 31$.

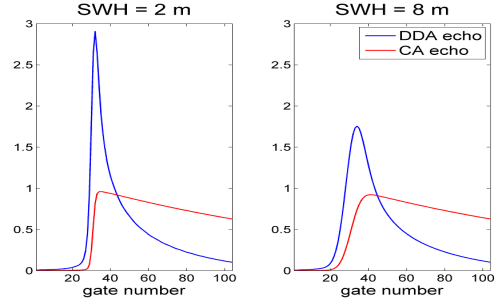


Fig. 2. Examples of delay/Doppler and conventional echoes for two values of SWH and $(\tau, P_u) = (31, 1)$.

3. CRAMÉR-RAO BOUNDS

3.1. Conventional altimetry

The observed altimetric signal s_c is corrupted by a multiplicative speckle noise distributed according to an exponential distribution [10]. In order to reduce the influence of this noise affecting each individual echo, a sequence of L consecutive waveforms is averaged on-board the satellite. Assuming pulse-to-pulse statistical independence and invoking the central limit theorem, the averaged signal can be written $y_c(k) = s_c(k) [1 + n(k)]$, for $k = 1, \dots, K$, where $n(k)$ is approximately distributed according to a zero mean Gaussian

distribution with variance $1/L$ i.e., $n(k) \sim \mathcal{N}(0, 1/L)$. An equivalent formulation is

$$y_c(k) = s_c(k) + n'(k), k = 1, \dots, K \quad (9)$$

where $n'(k) \sim \mathcal{N}(0, s_c^2(k)/L)$. Using (9) and assuming independence between the signal samples, the likelihood function of the vector of observations \mathbf{y}_c can be computed. It is the probability density function of a multivariate Gaussian distribution (denoted as $f(\mathbf{y}_c|\boldsymbol{\theta})$) with mean s_c and whose covariance matrix $\boldsymbol{\Sigma}(\boldsymbol{\theta}, L)$ is diagonal with diagonal elements $\Sigma_k(\boldsymbol{\theta}, L) = s_c^2(k)/L$, for $k = 1, \dots, K$. The Fisher information matrix (FIM) of the parameter vector $\boldsymbol{\theta}$ can then be computed by differentiating twice the log-likelihood function (see [8] for more details)

$$\mathbf{F}_c = \mathbf{D}_c^T \boldsymbol{\Sigma}^{-1}(\boldsymbol{\theta}, L + 2) \mathbf{D}_c \quad (10)$$

where \mathbf{D}_c is a $(K \times 3)$ matrix whose components are $D_c(k, i) = \frac{\partial s_c(k)}{\partial \theta_i}$, for $k = 1, \dots, K$ and $i = 1, \dots, 3$. The analytical expressions of these matrix components are not given in the present paper for space limitations but are available in a separate technical report [8]. Note that the proposed CRBs differ from those derived in [11] since the present paper considers the double convolution model (1) whereas the Brown model [6] was used in [11].

3.2. Delay/Doppler altimetry

Each Doppler beam has a size of about 300 meters which means that it is observed by the satellite during 43 ms (after taking into account the satellite velocity). Moreover, the satellite transmits 85 bursts of $N = 64$ pulses per second. As a consequence, each Doppler beam is observed by approximately 4 independent bursts, i.e., it is observed by $N_p = 256$ pulses. The observed discrete multi-looked echo can be expressed as

$$y_d(k) = \sum_{n=1}^N m(k, n) b(k, n) \quad (11)$$

where $m(t, f_n) = P(t - \delta t_n, f_n)$ denotes the signal of the n^{th} Doppler beam after delay compensation and $b(k, n)$ is an independent and gamma distributed speckle noise (whose shape and scale parameters equal 4) resulting from the average of 4 bursts. Invoking the generalized central limit theorem for sums of independent non-identically distributed random variables (e.g., the Lyapunov condition [12]), it makes sense to approximate the distribution of $y_d(k)$ by a Gaussian distribution whose mean is $\sum_{n=1}^N m(k, n)$ and whose covariance matrix $\boldsymbol{\Lambda}(\boldsymbol{\theta})$ is diagonal with diagonal elements $\Lambda_k(\boldsymbol{\theta}) = \frac{1}{4} \sum_{n=1}^N m^2(k, n)$, for $k = 1, \dots, K$. The FIM of the parameter vector $\boldsymbol{\theta}$ can then be computed leading to

$$\mathbf{F}_d = \mathbf{D}_d^T \boldsymbol{\Lambda}^{-1}(\boldsymbol{\theta}) \mathbf{D}_d + \mathbf{H}_d \quad (12)$$

where \mathbf{D}_d is a $(K \times 3)$ matrix whose components are $D_d(k, i) = \frac{\partial s_d(k)}{\partial \theta_i}$, for $k = 1, \dots, K$ and $i = 1, \dots, 3$ and \mathbf{H}_d is given by

$$H_d(i, j) = 2 \sum_{k=1}^K \frac{h_i(m, k) h_j(m, k)}{\left[\sum_{n=1}^N m^2(k, n) \right]^2} \quad (13)$$

where

$$h_i(m, k) = \sum_{n=1}^N m(k, n) \frac{\partial m(k, n)}{\partial \theta_i} \quad (14)$$

for $(i, j) \in \{1, 2, 3\}^2$. The analytical expressions of the partial derivatives of $m(k, n)$ with respect to P_u, τ and SWH are available in [8]. Note that the covariance matrix $\boldsymbol{\Lambda}(\boldsymbol{\theta})$ of the observed signal \mathbf{y}_d (which depends on the different signals $m(k, n)$) can be rewritten as a function of the multi-look echo s_d . For that purpose, an ‘‘effective number of looks’’ can be defined for the k th observation [9]

$$N_{\text{eff}}(k) = \frac{E^2[y_d(k)]}{E\{[y_d(k) - E(y_d(k))]\}^2} = \mu(k) N_p \quad (15)$$

where the components of the vector $\boldsymbol{\mu}$ are

$$\mu(k) = \frac{\left[\sum_{n=1}^N m(k, n) \right]^2}{N \sum_{n=1}^N m^2(k, n)} = \frac{s_d^2(k)}{N \sum_{n=1}^N m^2(k, n)}. \quad (16)$$

Note that $\mu(k)$ is smaller than 1 accounting for the fact that $N_{\text{eff}}(k)$ is smaller than N_p (see [9]). Using the previous notations, the k th diagonal element of the covariance matrix $\boldsymbol{\Lambda}(\boldsymbol{\theta})$ can be written $\Lambda_k(\boldsymbol{\theta}) = \frac{s_d^2(k)}{N_p \mu(k)}$, for $k = 1, \dots, K$. This expression is similar to the one obtained for CA (the number of looks L has been replaced by $N_p \mu(k)$ in the k th element of $\boldsymbol{\Lambda}$). Assuming a small variation of $\boldsymbol{\mu}$ with respect to the altimetric parameters, (i.e., $\frac{\partial \boldsymbol{\mu}}{\partial \theta_i} \approx \mathbf{0}$, for $i \in \{1, 2, 3\}$) leads to

$$\mathbf{F}_d \approx \mathbf{D}_d^T \boldsymbol{\Delta}^{-1}(\boldsymbol{\theta}) \mathbf{D}_d \quad (17)$$

where $\boldsymbol{\Delta}$ is a diagonal matrix with elements $\Delta_k(\boldsymbol{\theta}) = \frac{s_d^2(k)}{N_p \mu(k) + 2}$, for $k = 1, \dots, K$. Note that the FIM (17) has the same form as the one obtained for CA (10).

4. ESTIMATION METHODS

This section introduces the estimation methods considered in this study. The first method is based on the LS estimator that has received much attention in the literature [4,5]. The second method is based on the maximum likelihood principle which provides asymptotically efficient estimators. A third estimator constructed from a WLS criterion is finally investigated.

4.1. Least squares estimator

The LS estimator is classically defined as

$$\hat{\boldsymbol{\theta}}_{\text{LS}} = \underset{\boldsymbol{\theta}}{\text{argmin}} [\mathbf{y} - \mathbf{s}(\boldsymbol{\theta})]^T [\mathbf{y} - \mathbf{s}(\boldsymbol{\theta})] \quad (18)$$

where \mathbf{y} is the observed echo ($\mathbf{y} = \mathbf{y}_c$ for CA and $\mathbf{y} = \mathbf{y}_d$ for DDA), $\mathbf{s}(\boldsymbol{\theta})$ is the analytical waveform parameterized by

$\theta = (\text{SWH}, \tau, P_u)^T$ ($s(\theta) = s_c(\theta)$ for CA and $s(\theta) = s_d(\theta)$ for DDA). Since $s(\theta)$ is a complicated nonlinear function of SWH and τ , the optimization problem (18) does not admit a closed-form expression. In this paper, we propose to solve (18) using a numerical optimization method based on the Levenberg-Marquardt (LM) algorithm [13].

4.2. Maximum likelihood estimator

The maximum likelihood estimator (MLE) of θ denoted as $\hat{\theta}_{\text{ML}}$ is obtained by maximizing the likelihood function $f(\mathbf{y}|\theta)$ with respect to θ or by minimizing the negative log-likelihood. Straightforward computations show that the MLE of θ reduces to minimize the following cost function

$$\begin{aligned} \mathcal{C}(\theta) &= \ln[\det(\Omega(\theta))] + [\mathbf{y} - s(\theta)]^T \Omega^{-1}(\theta) [\mathbf{y} - s(\theta)] \\ &= \sum_{k=1}^K \ln[\Omega_k(\theta)] + \sum_{k=1}^K \frac{[y_k - s_k(\theta)]^2}{\Omega_k(\theta)} \end{aligned} \quad (19)$$

where $\Omega(\theta)$ is the covariance matrix of \mathbf{y} ($\Omega = \Sigma$ for CA and $\Omega = \Lambda$ for DDA). The MLE is asymptotically efficient and is thus expected to provide the smallest estimation variances. Unfortunately, the LM algorithm, which solves LS problems, cannot be applied to optimize (19) because of its form. In this study, we have optimized (19) using the Nelder-Mead (NM) algorithm [13].

4.3. Weighted least squares estimator

The MLE $\hat{\theta}_{\text{ML}}$ has nice asymptotical properties (it is asymptotically unbiased, convergent and asymptotically efficient) under mild assumptions. However, its application to delay/Doppler altimetry requires the use of an optimization algorithm (such as the NM algorithm) whose computational cost can be prohibitive [14]. An alternative is the WLS estimator defined as

$$\hat{\theta}_{\text{WLS}} = \underset{\theta}{\text{argmin}} [\mathbf{y} - s(\theta)]^T \Omega^{-1}(\theta) [\mathbf{y} - s(\theta)]. \quad (20)$$

An interesting property of this estimator is that the optimization problem (20) can be solved by using the LM algorithm (contrary to the optimization problem associated with the MLE). Note that a WLS estimator using a constant weighting matrix was proposed in [15]. The estimator (20) differs from this estimator since the weighting matrix $\Omega^{-1}(\theta)$ depends on θ . Motivations for using this weighting matrix can be found in [16].

5. SIMULATION RESULTS

The first experiments compare the square roots of the CRBs (RCRBs) obtained with CA and DDA in order to show the possible performance improvement when using the delay/Doppler concept. In a second step, we evaluate the performance of the three estimation algorithms introduced in Section 4 for DDA. This comparison is conducted by comparing the root mean square errors (RMSEs) of the different

estimators. The CRBs of the different parameters are also displayed to show whether there is some hope for improving estimation performance or not.

5.1. Comparison between CA and DDA

Fig. 3 shows the RCRBs of the three altimetric parameters for both CA and DDA when varying SWH in the interval [1, 8] meters. This figure shows a clear improvement for RCRB(τ) and RCRB(P_u) when considering DDA. For instance, for SWH = 2 m, we note an improvement by a factor of 1.7 for RCRB(τ) and by a factor of 1.28 for RCRB(P_u). It can also be observed that for small sea wave heights (i.e., SWH < 5 m), RCRB(SWH) is slightly higher for DDA than for CA. However, the possible improvement in the estimation of the epoch and amplitude is clearly of major importance.

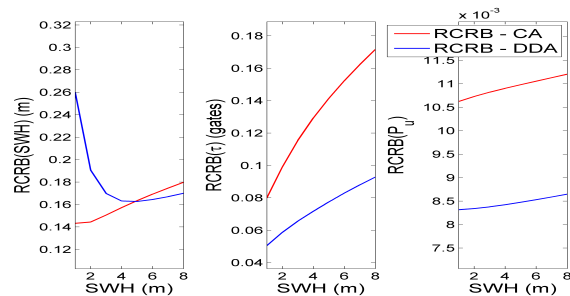


Fig. 3. RCRBs for delay/Doppler altimetry (DDA) and conventional altimetry (CA).

5.2. Estimation performance for DDA

Fig. 4 compares the RMSEs of the different estimators for the altimetric parameters (SWH (a), P_u (b) and τ (c)). The RCRBs are also displayed providing a reference in terms of estimation performance. The MLE and WLS perform very similarly. The LS estimator shows the worst performance when compared to the ML and WLS estimators. For instance, we can observe a gain of about 20 cm for SWH when using WLS or MLE instead of LS. The RMSEs of the WLS and MLE associated with the parameters SWH and P_u are very close to the corresponding CRBs showing there is no space for improving estimation performance for these two parameters. The situation is different for the epoch parameter since the RMSEs of the WLS and MLEs are 0.02 gates higher than the RCRBs. Thus, there is some space for developing better estimators for this parameter. This difference between the RMSEs of the MLE and the RCRBs can be explained by the fact the asymptotic region has not been reached for $K = 104$ samples.

Finally, it is interesting to mention that the computation cost of the WLS estimator is significantly smaller than that of the MLE. Indeed, estimating the parameters of a DDA waveform by the WLS method takes 7.4 seconds (with a MATLAB

implementation and a 2.93 GHz i7 CPU) whereas it needs 31 seconds for the MLE. This time reduction is mainly due to the formulation of the WLS that allows the use of the LM algorithm instead of the NM algorithm. Note also that the LS algorithm is the fastest algorithm (2.6 seconds for estimating the parameters of a waveform) but it shows reduced performance because it does not take into account the nature of the noise and in particular the structure of the noise covariance matrix.

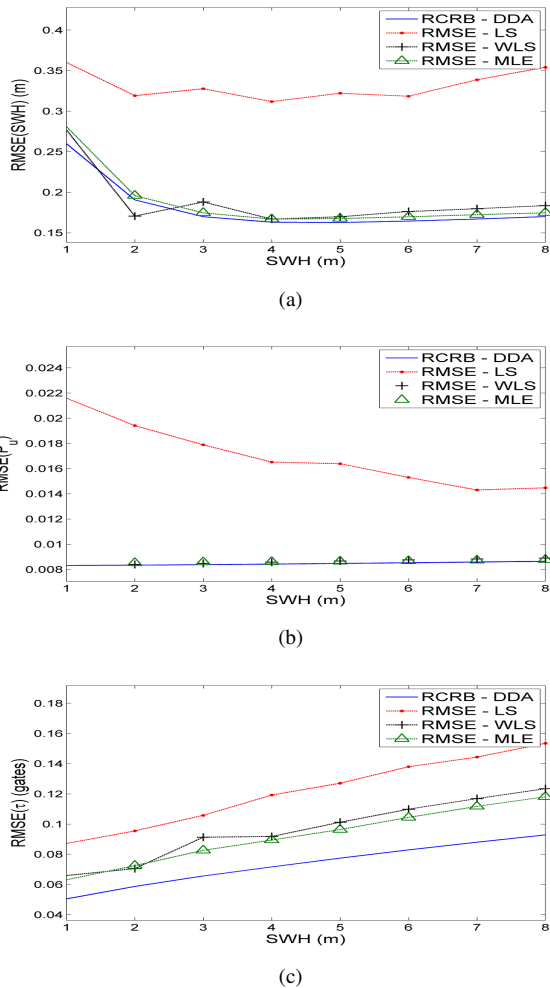


Fig. 4. RCRBs and RMSEs for the LS, WLS and ML algorithms.

6. CONCLUSIONS

This paper derived the Cramér-Rao lower bounds for the parameters of the double convolution model for radar altimetry. This model has received a considerable attention for conventional altimetry whereas its application to delay/Doppler altimetry is more recent. The analysis of these Cramér-Rao bounds has confirmed that an improved estimation performance can be expected when using delay/Doppler altimetry (especially regarding the amplitude and the epoch of the altimetric waveform) instead of conventional altimetry. The gain

in estimation performance for the sea wave height strongly depends on the value of this parameter due to the shape of the delay/Doppler echo. Another contribution of this work is the derivation of a new weighted least-squares algorithm which combines the advantages of the least squares algorithm (small computational cost) and of the maximum likelihood estimator (high estimation performance). Prospects include the analysis of the correlations between the estimated altimetric parameters. Extending the CRBs to a more general model including other altimetric parameters (such as antenna mispointing) is also an interesting issue. These points are currently under investigation.

7. REFERENCES

- [1] R. K. Raney, "The delay/Doppler radar altimeter," *IEEE Trans. Geosci. and Remote Sensing*, vol. 36, no. 5, pp. 1578–1588, sep 1998.
- [2] A. Halimi, C. Mailhes, J.-Y. Tourneret, F. Boy, N. Picot, and P. Thibaut, "An analytical model for Doppler altimetry and its estimation algorithm," in *Ocean Surface Topography Science Team Meeting*, Venice, Italy, September 2012.
- [3] A. Halimi, C. Mailhes, J.-Y. Tourneret, P. Thibaut, and F. Boy, "A semi-analytical model for delay/Doppler altimetry and its estimation algorithm," 2012, submitted.
- [4] E. Rodriguez, "Altimetry for non-Gaussian oceans: height biases and estimation of parameters," *J. Geophys. Res.*, vol. 93, pp. 14,107–14,120, 1988.
- [5] L. Amarouche, P. Thibaut, O. Z. Zanife, J.-P. Dumont, P. Vincent, and N. Steunou, "Improving the Jason-1 ground retracking to better account for attitude effects," *Marine Geodesy*, vol. 27, pp. 171–197, 2004.
- [6] G. Brown, "The average impulse response of a rough surface and its applications," *IEEE Trans. Antennas and Propagation*, vol. 25, no. 1, pp. 67–74, jan 1977.
- [7] C. Martin-Puig and G. Ruffini, "SAR altimeter retracker performance bound over water surfaces," in *IGARSS-09*, vol. 5, South Africa, july 2009, pp. V-449–V-452.
- [8] A. Halimi, C. Mailhes, and J.-Y. Tourneret, "Cramér-rao bounds and estimation algorithms for delay/Doppler and conventional altimetry," University of Toulouse, France, Tech. Rep., March 2013. [Online]. Available: <http://halimi.perso.enseeiht.fr/>
- [9] D. Wingham, L. Phalippou, C. Mavrocordatos, and D. Wallis, "The mean echo and echo cross product from a beamforming interferometric altimeter and their application to elevation measurement," *IEEE Trans. Geosci. and Remote Sensing*, vol. 42, no. 10, pp. 2305 – 2323, oct. 2004.
- [10] C. Oliver and S. Quegan, *Understanding Synthetic Aperture Radar Images*. London: Artech house publishers, 1998.
- [11] C. Mailhes, J.-Y. Tourneret, J. Severini, and P. Thibaut, "Cramér-rao bounds for radar altimeter waveforms," in *EUSIPCO-08*, lausanne, Switzerland, 28 August 2008.
- [12] P. Billingsley, *Probability and Measure*, 3rd ed. United States of America: John Wiley & Sons, Inc., 1995.
- [13] D. P. Bertsekas, *Nonlinear programming*. Belmont, Massachusetts: Athena Scientific, 1995.
- [14] A. Halimi, C. Mailhes, J.-Y. Tourneret, P. Thibaut, and F. Boy, "Parameter estimation for peaky altimetric waveforms," *IEEE Trans. Geosci. and Remote Sensing*, vol. 51, no. 3, pp. 1568–1577, march 2013.
- [15] L. Phalippou and V. Enjolras, "Re-tracking of SAR altimeter ocean power-waveforms and related accuracies of the retrieved sea surface height, significant wave height and wind speed," in *Geoscience and Remote Sensing Symposium, 2007. IGARSS 2007. IEEE International*, july 2007, pp. 3533–3536.
- [16] B. Porat and B. Friedlander, "Performance analysis of parameter estimation algorithms based on high-order moments," *Int. J. Adapt. Control Signal Process*, vol. 3, no. 3, pp. 191–229, September 1989.